Incorporation of Copper/Melamine Complexes in Silica Surface and Their Sorption Activity of Organic Dye

Elsharkawy, Rehab G.*[+•]

Chemistry Department, Faculty of Science, Tanta University, Tanta, EGYPT

ABSTRACT: *The efficiency and performance of supported melamine/ copper complexes, S/[$CuCl_2(Mel)_2$].2MeOH, as a new adsorbent, for the adsorptive removal of Indigo Carmine (IC) from aqueous solutions, has been evaluated with respect to several experimental conditions including contact time, initial IC concentration, temperature and adsorbent dosage. The maximum removal percentage (approximately 84%) was observed when used 0.05 g/L of S/[$CuCl_2(Mel)_2$].2MeOH, 1.5 x 10^{-5}mol/L of initial IC concentration and contact time of 15min. The experimental data were analyzed by the Langmuir, Freundlich, and Tempkin isotherm models. The monolayer adsorption capacity of S/[$CuCl_2(Mel)_2$].2MeOHwas found to be 16.8 x 10^{-3}mol/g by using Langmuir isotherm model. The calculation of the thermodynamic parameters such as Gibbs free energy, entropy and enthalpy changes of the ongoing adsorption process indicated the feasibility and endothermic nature of IC adsorption. The kinetics study suggested that the adsorption of IC onto S/[$CuCl_2(Mel)_2$].2MeOH proceeds according to the pseudo-second-order model.*

KEYWORDS: *Melamine complexes; Characterization; Removal; Adsorption; Indigo carmine*.

INTRODUCTION

Melamine (MA; 1, 3, 5- Triazine- 2, 4, 6- triamine) is a kind of Triazine analog with three amino groups and it can be also described as a trimer of cyanamide [1]. MA has been exhibited diversified hydrogen bonding modes and extremely interesting architectures [2- 5]. MA can be hydrolyzed into ammeline, ammelide, and cyanuric acid under acidic or alkaline conditions (Scheme 1): the dissociation constant (pK_a) for melamine is 5.0 [6].

Melamine was mainly used to produce melamine formaldehyde resins for surface coatings laminates, adhesives, plastics, molding compounds, kitchenware, and flame retardant materials [7- 10]. MA that can recognize the donation and acceptance of hydrogen bonds, metal chelation, and π- π interactions, have been proven great potential in the rising areas of supermolecular [11, 12] and dendrimer [13] chemistry. Several melamine complexes have been reported [14- 18]. *Lu et al.* [19] have demonstrated that MA is capable of cheating to the Zn II center to form a luminescent complex. The reactions of $CuCl_2$. 2 H_2O and $Cu(OAC)_2$. H_2O in a boiling methanol solution afforded two Cu II complexes [2]. Also, coordination of Cu (I) and Cu (II) salts to melamine produces [Cu X (MA)] where X = Cl, Br, I, or NO_3, [Cu X_2 $(MA)_2$]. S, [X= Cl, Br, or OAC, S= H_2O, or 2 MeOH] have been reported [16]. *Schwab et al.* developed a class of high-performance porous polymer networks, namely Schiff base networks (SIVW), with a high surface area by condensation of MA with several

***** *To whom correspondence should be addressed.*

+ *E-mail: relsharkawy@yahoo.com*

Other Address: Chemistry Department, Faculty of Science, Aljouf University, Kingdom of Saudi Arabia (Box No. 2014)

1021-9986/2017/5/99-114 16/$/6.60

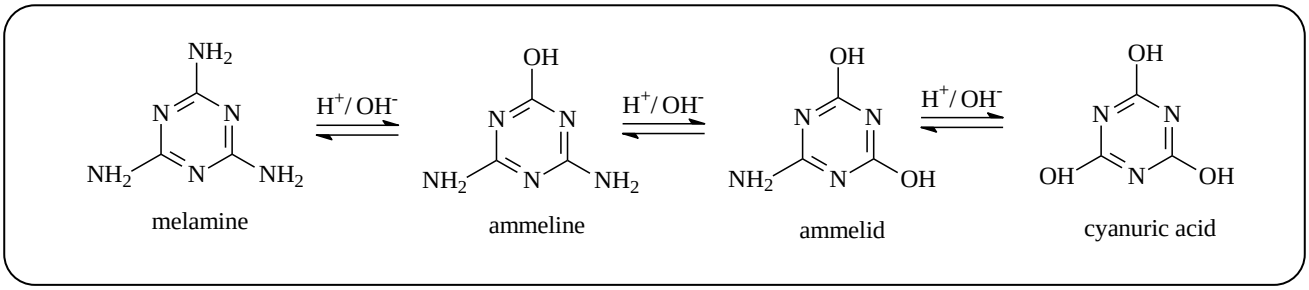

Scheme 1: The hydrolysis reaction of melamine under acidic and alkaline conditions.

aromatic aldehydes through Schiff base chemistry in DMSO [20]. Huang et al [21] have been synthesized two Ag(I) Coordination Polymers (CPs) constructed from melamine and the dicarboxylic acid. Based on the unique electronic properties and high adsorption capacity of carbon nanotubes as well as the electrostatic attraction between protonated melamine and negatively charged bisphenol A (BPA), a novel electrochemical sensor for the determination of BPA in water was fabricated by immobilization of MultiWall Carbon Nano Tubes (MWCNTs) / melamine complex onto the surface of glassy carbon electrode [22].

Indigo Carmine (IC) is one of the oldest dye used mostly for cotton clothes dyeing (blue jeans) [23]. The wastewater-containing indigo is characterized by a dark blue color due to cross-conjugated system or H-chromophore, consisting of a single –C=C– double bond substituted by two NH donor groups and two CO acceptor groups. It is considered as a highly toxic dye that can cause skin and eye irritations [24]. It is also known to cause mild to severe hypertension, cardiovascular and respiratory effects in patients [25]. Discharges of untreated dye effluent into the water body produce colored effluents that not only cause esthetic deterioration but also affect oxygen and nitrogen cycles through photosynthesis, and they may also be toxic to aquatic biota [26].Therefore, the residue of indigo dye-containing wastewater, especially textile effluent, must be treated before being discharged safely into a water body[27-29]. Several processes have been suggested for removal of Indigo Carmine. The decolorization of the indigo carmine dye was investigated by various advanced oxidation technologies, such as Fenton reagent [30], electrochemical oxidation [31] and photoassisted oxidation [32].

The present study was undertaken to evaluate the efficiency of supported melamine/ metal complexes powder as an adsorbent for the removal of IC dye from aqueous solutions. The kinetic, equilibrium and thermodynamic data on batch adsorption studies were carried out to understand the process of adsorption. The effect of adsorption parameters such as initial dye concentration, temperature, adsorbent dose, contact time has been studied. This model system may be applicable to color removal in a textile wastewater stream.

EXPERIMENTAL SECTION

Materials and methods

All reagents were commercially available and used as received. Silica (60-120 mesh) with particle size 0.063-0.2 mm was obtained from Baker. It has an estimated surface area of200 m^2/g. Silica-alumina (25% Al_2O_3) was obtained from Joseph Grossfield&Son. Ltd and used as received. It has a pore volume of 0.8 cm^3/g, the average particle size of 63 μm and surface area of 250 m^2/g as determined by high-speed surface area Analyzer(Shimadzu, model 2205). Indigo Carmine (IC) dye (disodium salt of 3, 3- dioxobi- indolin- 2, 2- ylidine- 5, 5- disulfonate),was obtained from Aldrich, (Scheme 2). Copper chloride, copper sulfate, copper acetate, and melamine were supplied from El-Nasr Chemicals Co. (ADWIC, Egypt). The morphology of the complexes was examined by Scanning Electron Microscope (SEM), Hitachi FL-SEM "S-800". X-ray diffraction patterns were measured by using an MXP-18 diffractometer (Mac science Co. Ltd) with monochromatic CuKα radiation. Infrared spectra were recorded on an FT-IR spectrophotometer (Perkin-Elmer 1430) to identify the chemical structure of the complexes. The KBr technique was used to prepare FTIR test samples. Elemental analysis of the complexes was made by Perkin-Elmer 2400elemental.

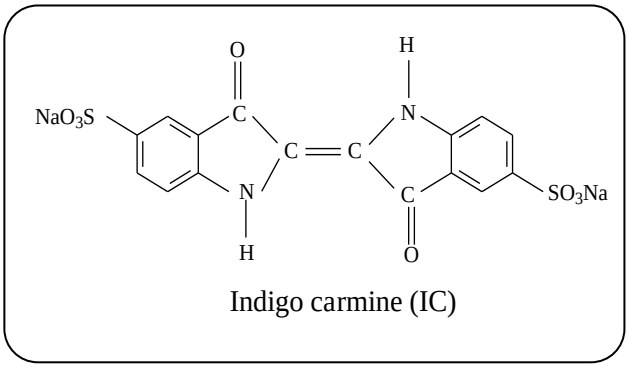

Indigo carmine (IC)

Scheme 2: Indigo Carmine dye (IC).

Synthesis

The melamine complexes and supported melamine complexes were prepared by the same procedure. 1.36 g (2.53x 10^{-3}mole) of $CuCl_2$. $2H_2O$ had been dissolved in the solution of 1.0g (1.98x 10^{-3} mole) melamine in 40 mL CH_3OH. The mixture was heated to reflux for 3 h until some green-yellow solid started to precipitate. The mixture was then permitted to stir for 1 h at room temperature. The solid was filtered out**,** washed with methanol, the products were dried overnight. Exactly the same procedure applied for supporting melamine/metal complexes by adding 3 g of silica or silica-alumina.

Kinetic measurements

The interaction between Melamine complexes and supported melamine complexes with the IC was monitored spectrophotometrically using a Shimadzu 2100S UV/Vis double beam recording spectrophotometer. 0.04g of copper-melamine complexes was transferred into a number of conical flasks (100 mL) followed with distilled water (8.5 mL). The flasks were mounted in a temperature controlled water bath with shaking facility to attain the desired temperature (30 ± 0.1ºC). Into each flask 1.5ml of thermostated stock solution of the IC (1 x 10^{-3} mol/L) were added and the time was noted. The concentration of IC in the reaction mixture was thus $1.5x10^4$ mol/L. The heterogeneous reaction mixtures were immediately shaken by mild shaking speed (120 rpm) during the span of reaction time without possible mass transfer to the wall of the flask. To examine the progress of dye removal, the flasks were taken from the water-bath in turn at appropriate intervals and the solutions were pipetted out for the UV/Vis measurements, whereby the concentration of the remaining dye in solution was determined.

RESULTS AND DISCUSSION

Morphology of the complexes

Scanning Electron Microscope (SEM) technique gives a broad perception of surface morphology, microstructure particle size, and chemical composition. Scanning Electron Micrographs (SEM), Fig. 1, were obtained in the copper- melamine complex and S/$[CuCl_2(Mel)_2]$.2MeOHin order to detect differences in their surfaces. SEM of both samples was obtained at 500 magnifications. SEM image of copper- melamine complex is composed of various irregular- shaped microparticles, exhibited an "eroded rock" like surface. While SEM of S/$[CuCl_2(Mel)_2]$.2MeOH was displayed to clarify the agglomeration for the Cu-melamine particles after supporting on silica. The loaded functional groups were distributed on the whole surface that made the surface of the product S/$[CuCl_2(Mel)_2]$.2MeOH become rough

Elemental analysis

The results of elemental analysis obtained for melamine complexes were performed and tabulated in Table 1. The theoretical values of elemental analysis showed a good agreement with the experimental values. There is about 1% difference between calculated and experimental data. This can be attributed to the drastic complexation conditions utilized.

FT-IR spectra

The wavenumber positions of transmission peaks, peak intensities, and peak widths are helpful for the functional group and sample identification. Wave number positions of transmission bands are specific towards the functional groups in a sample; thus, each sample has a distinctive fingerprint absorbance spectrum.

The FT-IR spectra of melamine are definitely known and it has now been reinterpreted fairly recently [16, 33, 34]. The presence of melamine is shown by absorptions at 3468, 3418, 3333, 1,650, 1,576, 1,461, 1,026, and 816 cm^{-1} using its IR spectrum (Fig. 2), which will be most typical of melamine IR (Table 2) [35- 37]. The IR transmission peaks at 3500–3000 and 1700–1300 cm^{-1} in the melamine, spectra are associated with the stretching

Table 1: The elemental analysis data for the supported and not- supported Cu- melamine complex.

Compound	C%		H%		N%	
	Cal.	Found	Cal.	Found	Cal.	Found
$[CuCl_2(Mel)_2].2MeOH$	18.61	18.88	3.99	3.95	28.94	29.28
$[CuSO_4(Mel)_2].2MeOH$	18.06	18.49	2.70	2.90	21.32	22.24
$[Cu(OAC)_2(Mel)_2].2MeOH$	14.64	15.14	4.37	4.22	24.57	25.46

Table 2: Characteristic absorption bands (cm-1) of supported and not- supported Cu- melamine complex.

Compound	$(—NH_2^+)_{st}$	$(—NH_2^+)$ asymmetric	NH deformation	$(C\text{-}N^{+\cdot})$	Absorption of triazine ring	Cu-N vibration
Melamine	3468, 3418	3333	1650	1026	1570, 1461, 816	-
$[CuCl_2(Mel)_2].2MeOH$	3444	3359	1681	1024	1541, 1468, 805	469
$S/[CuCl_2(Mel)_2].2MeOH$	3444	3356	1683	1021	1540, 1464, 813	471
$S\text{- }Al/[CuCl_2(Mel)_2].2MeOH$	3445	3360	1660	1025	1549, 1465, 874	466

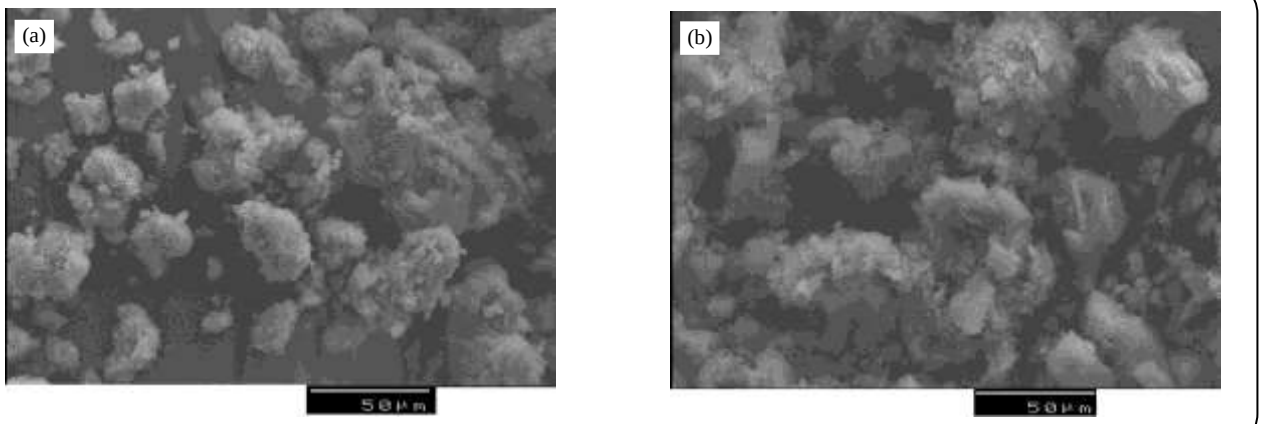

Fig. 1: Scanning electron micrographs: (a) Cu- melamine complex particles and (b) S/Cu- melamine complex.

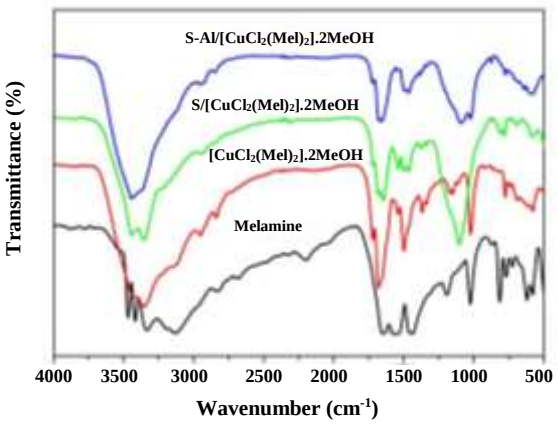

Fig. 2: FT-IR spectra of supported and not- supported Cu (II) – melamine complexes.

and bending vibrations of amino groups contained in the melamine, respectively. The absorptions at 3468 and 3418 cm^{-1} are assigned to NH_2 stretching vibrations that would be the typical feature of melamine. The peak at 3333 cm^{-1} is related to asymmetric stretching absorption of N–H, while the peak at 1650 $cm^{-1}$is assigned to deformation vibrations for the N–H group [38, 39]. The peaks at 1576, 1461and 816 cm^{-1} are assigned to absorptions of triazine rings [40]. The 1026 cm^{-1} peak is an outcome of C–N stretching vibration [28].

The spectra of melamine are compared to those associated with the $S/[CuCl_2(Mel)_2].2MeOH$complexes, Fig. 2. The main chemical groups present in the silica and silica-alumina were identified by FT-IR spectra [41]. The broadband at 3444$cm^{-1}$to 3445 cm^{-1} is caused by

the stretching vibration from the O-H bond through the silanol groups (SiOH) in silica and silica-alumina respectively, that will also result from the adsorbed water molecules on the silica surface [42,43]. The band at 1105 cm^{-1} to 1093cm^{-1} is the result of the Si-O-Si asymmetric stretching vibration, while the band at 782 cm^{-1} to 776 cm^{-1} has been assigned to the network Si-O-Si symmetric bond stretching vibration [43]. The band at 467cm^{-1} refers to the stretching vibration of Cu- N bond.

In comparison to free Melamine, the spectra of supported melamine complexes exhibit some new peaks including the Cu-N bond at 467 cm^{-1} and the Si-O-Si asymmetric stretching vibration at 1105 cm^{-1}.

X-ray diffraction

X-ray powder diffraction analysis was used to simply help characterize the newest products. Sharp line diffractograms were obtained in most cases, indicating good sample crystallinity. X-ray powder diffraction of MA was compared to those of Cu- melamine complex and S/[$CuCl_2$(Mel)$_2$].2MeOH, Fig 3. The intense peaks of free MA at 2θ = 26° has the same profile when compared with MA in the literature [42]. The XRD patterns for the three samples i. e.Cu- melamine complex, silica/ Cu-melamine complex, Si-Al_2O_3/ Cu- melamine complex, show remarkably different diffraction peaks and relative intensities, indicating they've been products with compositions distinct from melamine. The diffractogram from the material provisionally recognized as Cu- melamine complex appeared to be distinct from those of melamine. The intense peak at 2θ = 10 is characterized peak of Cu- melamine complex, moreover, the XRD of silica/ Cu- melamine complex revealed that the distortion in the crystal structure of Cu- melamine complex has occurred during preparation in presence of silica. The broad X-ray diffraction pattern is typical of the amorphous silica solid at 2θ = 22 [42].

Differential thermal analysis (DTA)

The DTA thermograms of pure melamine and melamine complexes were recorded under the same measurement conditions. As shown in Fig. 4. It absolutely was found that the decomposition of melamine in nitrogen contains two or more processes. In line with the publications [36], the evaporation competes with the condensation of melamine in the temperature range

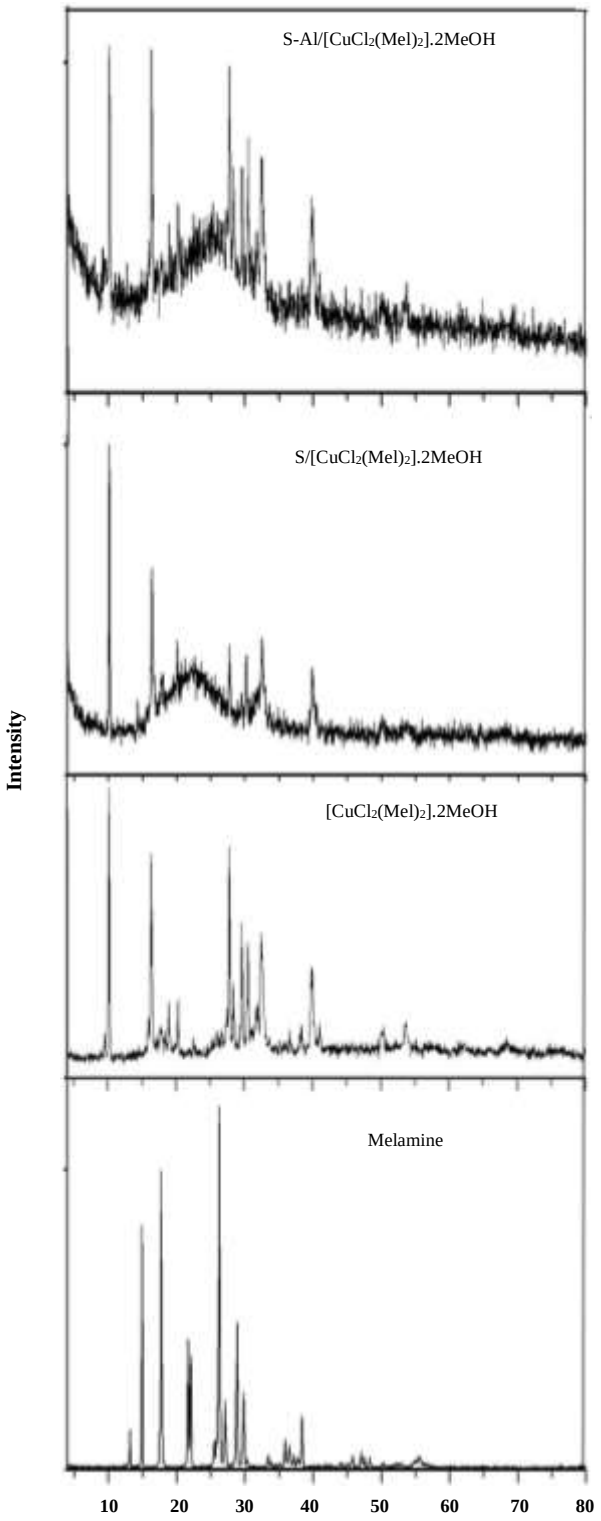

Fig. 3: X-Ray powder diffraction for copper melamine complexes.

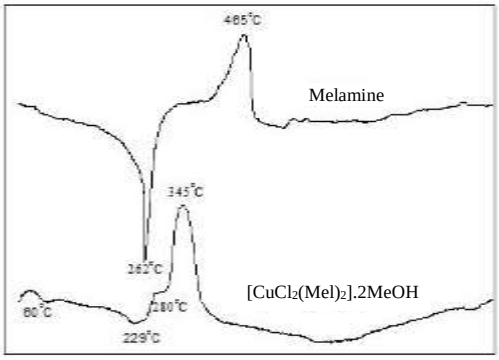

Fig. 4: DTA traces for melamine and Cu- melamine complex.

250–380ºC, that leads to the formation of melam, melem, and melon accompanied with the elimination of ammonia, plus also the residue from the decomposition of melamine at 400ºC continues to decompose at high temperatures. Schnick et al. have proven that melamine can condense into different intermediates and release ammonia at different temperatures, respectively [44, 45]. Several important intermediates such as melam ($(C_3N_3)_2(NH_2)_4(NH)$), melem ($C_6N_7(NH_2)_3$), melon ($(C_6N_7)_3(NH_2)_3(NH)_3$). It had been stated that the condensation products are more thermally more stable than melamine, in other words, "melam stable to 350ºC, melem to 450ºC, and melon to 600ºC"[46]. Therefore, it could be postulated from our study that we now have much fewer amounts of later two products, i.e. melem and melon formed through the decomposition of melamine since it degrades nearly completely at about 400ºC.

The DTA curves indicate that the thermal decomposition of melamine complexes broadly involves three stages, [47]; *viz* dehydration (in case of hydrated one), deamination and deanionation. The dehydration process is generally found to spread over somewhat large temperature intervals leading to broad steps; while the deamination steps in practically most of the cases are quite steep ranging over an interval of just a few degrees. In most cases, the last steps were comprised of and its with simultaneous oxidation of Cu to CuO. The DTA of Cu-melamine complex exhibit a weak and somewhat broad endothermic peak in the lower temperature region corresponds to the loss of crystal water at 50ºC (in case of hydrated complexes) the endothermic nature of these DTA curves implies some kind of phase change associated with an absorption of the required latent heat. The exothermic peaks at 280 and 345ºC were results from the decomposition of melamine. The DTA peaks for deamination and deanionnation and conversion of metallic Cu to CuO processes are typical exothermic in nature. However, there is no distinct peak corresponding to the last process of oxidation of metallic Cu to CuO since it occurs almost simultaneously with the deanionation. The DTA peaks for the Cu to CuO process are rather weak and spread over a broad temperature range (400- 600ºC).

$$\underset{\text{(endothermic)}}{\text{phase change}} \longrightarrow \underset{\text{(endothermic}}{\text{Dehydration}} \longrightarrow \underset{\text{(exothermic)}}{\text{Deamination}}$$

$$\longrightarrow \underset{\text{(exothermic)}}{\text{Deanionation}} \longrightarrow \text{Cu} \xrightarrow{[O]} \text{CuO}$$

$$CuL_2X_2 \cdot nH_2O \xrightarrow[\text{dehydration}]{-xH_2O} CuL_2X_2 \xrightarrow[\text{deamination}]{-yL}$$

$$CuX_2 \xrightarrow[\text{deanionation and oxidation}]{-zX+O} CuO$$

Adsorption experiments

As soon as the IC was charged towards the supported/ Cu- melamine complexes, a fast drop in the absorbance of the dye was noticed in the first minute of contact. The absorbance then continued to decrease gradually with the lapse of the time (Fig. 5). Such a decrease in absorbance was accompanied by color removal over the period of contact which sometimes extended to 2 h. in this period the absorbance of IC was declined to ca. 80-85 % of these original values, based on the reaction conditions applied. The rate of color or dye removal was a function of several factors. In order to investigate these factors, the kinetics of supported/ Cu- melamine complexes/IC interaction was performed. The UV/Vis absorption spectra of dye solution were recorded in the range 200-800 nm. The concentration of residual dye in solution was calculated from the extinction coefficient (ε = 16365 L/mol cm) determined experimentally from the standard Beer-Lambert plot at λ_{max} = 610nm.The adsorbed amount (Mol/g) of indigo dye at time t, q_t, was calculated from the mass balance equation,

$$q_t = (C_o - C_t)\, V / m \qquad (1)$$

Where C_o and C_t are the initial and liquid-phase concentrations of dye solution (Mol/l) at time *t*, respectively. *V* is the volume of solution (L), and m is the mass per gram of silica/ Cu- melamine complex.

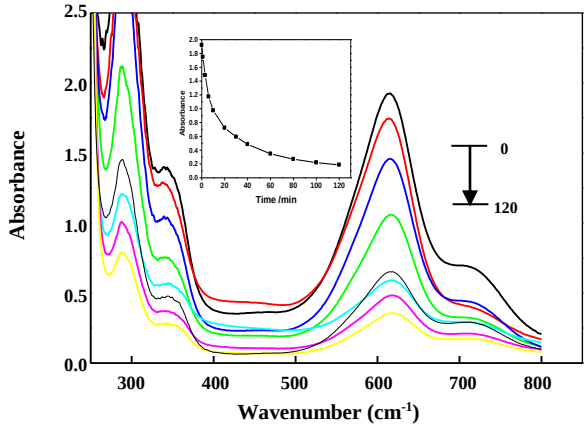

Fig. 5: Absorbance traces with time for IC when brought into contact with Cu- melamine complexes. [IC] = 1.5 x 10^{-4}mol/L, complex wt = 0.04 g.

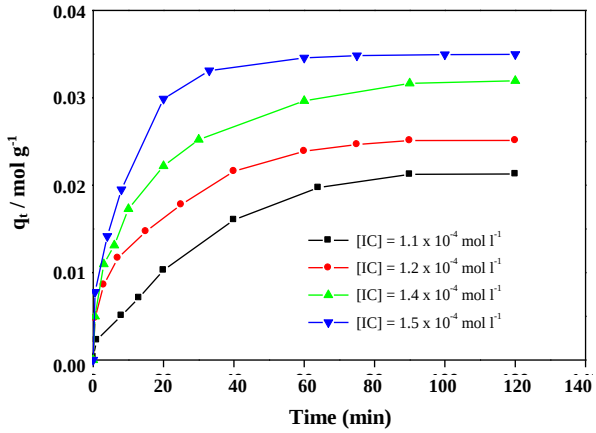

Fig. 6: Effect of initial concentration and time on IC adsorption by S/ Cu- Melamine complex

Adsorption isotherms were established with 0.04gofsilica/ Cu- melamine complex and the [IC] within the range of 1x 10^{-6}–2x10^{-5}mol/L. The experiments were carried out at 25, 30, 35, and 40°C in a temperature-controlled shaking water bath to evaluate the equilibrium constant (K_c) as well as the corresponding thermodynamic parameters.

Effect of contact time

The adsorption of IC dye onto silica/ Cu- melamine complex as a function of contact time is represented in Fig. 6. Fast adsorption was noticed in the initial 15 min accompanied by a gradual decrease in the adsorption rate until the adsorption reaches the equilibrium state in about 100 min. The full time needed to attain the state of equilibrium is termed the equilibrium time. The adsorbed amount of the dye in the equilibrium time reflects the adsorption capacity of the adsorbent under certain operating conditions [48- 50].Short equilibrium time indicates a higher surface area of the adsorbent and its suitability for fast and quantitative removal of dye. It had been found that the adsorption rate is rapid during the initial stages (probably related to the high ratio of the vacant site to adsorbate molecule), in addition, the system reaches equilibrium in about 10 min. The rapid adsorption in the initial contact time may be attributed to the availability of the reactive site of adsorbent, while at the higher time results from the slow pore diffusion or saturation of adsorbent the removal rate does not change. As it is obvious, significantly that more than 80% of IC removal was achieved in 8 min and thereafter the adsorption rate is slow so that up 98% of IC removal occurs at 10 min. It seems that at the lower time due to the high concentration gradient of IC its removal rate is high and sharp.

The adsorption curves were single, smooth and continuous up to the saturation state indicating the possible formation of monolayer coverage on the surface of adsorbent by the dye molecules [51]. This is due to the strong attractive forces involving the dye molecules and the adsorbent surface.

intraparticle (2) was obtained.

$$\frac{1}{C} = \frac{1}{C_0} + k_0 t \qquad (2)$$

C_o and C are the initial concentration and the concentration in solution at time t of IC in mol/L. k_o is the pseudo-second-order rate constant determined from the slope of the linear regression plot of Eq. (2), which was chosen to characterize each supported Cu- melamine complexes /IC interaction under any specific conditions. The effects of the above various variables are then discussed below in some details

Effect of initial dye concentration

The influence of IC initial concentration within the range of 1 x10^{-4} M –1.5 x 10^{-4}mol/L on its removal percentage and the actual amount of adsorbed dye

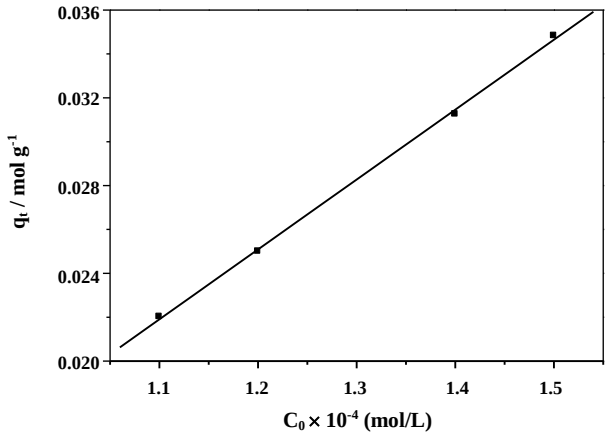

Fig. 7: Dependence of adsorbed amount of IC dye onto S/ Cu-Melamine complex at equilibrium on its initial concentration at 30°C.

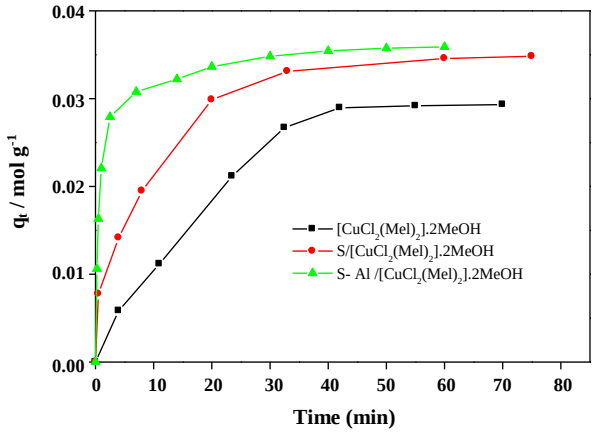

Fig. 8: The pre-equilibrium amount of IC dye adsorbed onto different supported Cu-Melamine complexes 30°C.C_o = 1.5 x 10^{-4}mol/L.

was investigated and results are shown in Fig. 7. At higher concentration of IC regardless of the actual amount of adsorbed IC, the removal percentage probability due to saturation of adsorbents surface significantly increase. The high adsorption capacity and fast adsorption procedure could be related to the high tendency of the soft atom of adsorbents to a soft atom of the IC through ion-dipole interaction or hydrogen bonding of IC molecules with different functional groups of melamine complexes.

Effect of adsorbent dosage

The adsorbent dose is an important parameter in the adsorption studies because it determines the capacity of the adsorbent for a given initial concentration of dye solution. It has been observed that the removal percentage increased rapidly with the increase in the adsorbent dose. This may be attributed to the increase in the adsorbent surface area and availability of more active adsorption sites on the supported / melamine complexes surface with increasing the dosage of the adsorbent.

Effect of temperature

The temperature influence is an important controlling factor in the real applications of the proposed adsorptive dye removal process since most of the textile dye effluents are produced at relatively high temperatures. In order to determine whether the ongoing IC adsorption process was endothermic or exothermic in nature, a set of similar experiments was carried out in the temperature ranges of 298-313 K at a constant initial dye concentration of 1.5 x 10^{-4}mol L^{-1} and the adsorbent dose of 0.04 g. The results showed that the adsorption amount of IC onto supported/melamine complexes increased from 31 to 40mg/g with an increase in temperature indicating that the process is endothermic in nature. The increase in the adsorption capacity of supported/ melamine complexes with temperature may be the results of the increase in the mobility of dye molecules and also increase in the number of available active surface sites on the supported / melamine complexes for adsorption as a result of pore enlargement.

Effect of support and dopant anion

The effect of the surface type has also been investigated using copper melamine complex itself and supported on silica-alumina (25% Al_2O_3), and silica. The dependence of the reaction rate on the supporting surface followed the order: silica-alumina > silica>copper melamine complex, Fig. 8. generally, the amount of complex adsorbed on the various solids has been correlated to the point of zero charges (pzc) of the surface that equals 8.5 and 1.9 for silica-alumina, and silica, respectively [52]. This reveals that the adsorption of the complex requires an electrostatic interaction between the complex and the hydroxyl groups on the supporting surface. Therefore, the difference in the adsorption mode of the surface produces changes in the amount of the complex.

On the other hand, For the Cu (II) complexes, the reaction rate is strongly influenced by the kind of the coordinated anion (Fig. 9).The dependence of the reaction rate on the type of the anion followed the order: CH_3COO^- >Cl^-> SO_4^{-2}. This order of rate constant may be ascribed to the following effects: (i) The difference of the reactivity of Cu (II) complexes could be attributed to the redox potential of every Cu(II) ion in the copper(II) complexes. Since the redox potential of the Cu (II) ion is considered to be affected by the coordination structure [53], (ii) Also, The difference of reactivity might be due to the selectivity order of those anions toward the adsorption on the oxide surface. It was reported that the acetate anion is a highly preferable adsorbed anion, while sulfate anion may be the lowest one. (iii) the crystallographic radii of those acids anions that are somewhat different with values; 0.27 nm, 0.16 nm, and 0.18 nm for SO_4^2 , OAC^-, Cl^-, and NO_3^-, respectively [54, 55]. (iv)The shape of these anions, which is also remarkably different; SO_4^{-2} is tetrahedral, Cl^- is spherical, while acetate is trigonal planar [54]. Obviously, these differences must have some influence on the crystallinity of the prepared composites.

Adsorption equilibrium study

Adsorption isotherms are essential to understand the nature of the interaction between the adsorbate and the adsorbent employed for the removal of pollutants [56]. An adsorption isotherm describes the relationship between the number of adsorbate uptakes by the adsorbent and the adsorbate concentration remained in the solution [57,58]. There are many equations for analyzing the experimental adsorption equilibrium data. The equation parameters of those equilibrium models often provide some insight into the mechanism, the surface properties of an adsorbent and affinity of the adsorbent for an adsorbate [58–60].

Although several isotherm equations have been developed, three important models, Langmuir, Freundlich and Temkin isotherms, were applied in this study. The Langmuir isotherm is based on the assumption that the adsorption process takes place at specific homogeneous sites within the adsorbent surface and that once a dye molecule occupies a site, no further adsorption can take place at that site, which concluded that the adsorption process is a monolayer in nature. The model is represented in the linear form as follows [60];

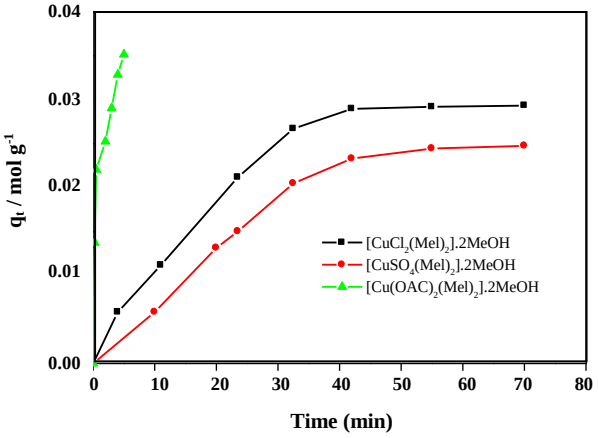

Fig. 9: The pre-equilibrium amount of IC dye adsorbed onto different Cu-Melamine complexes 30°C. C_o = 1.5 x 10^{-4}mol/L.

$$C_e/q_e = 1/K_L Q_{max} + Ce/Q_{max} \quad (3)$$

where K_L (L/mg) is the Langmuir isotherm constant related to the free energy or net enthalpy of adsorption and Q_m (mg/g) is the theoretical maximum adsorption capacity. The values of Q_m and K_L constants and the correlation coefficients for Langmuir isotherm are presented in Table 4. The isotherms of the adsorption of IC onto supported / melamine complexes were found to be linear over the whole concentration range studies with high correlation coefficients (R^2 > 0.99). The Freundlich isotherm, derived by assuming a heterogeneous surface with a non-uniform distribution of sorption heat over the surface, is presented in the linear form as follows [61];

$$\log q_e = \log K_F + 1/n \log C_e \quad (4)$$

Where K_F (mg/g) is the constant related to the adsorption capacity, and *n* is the empirical parameter related to the intensity of adsorption. The value of n varies with the heterogeneity of the adsorbent and in the favorable adsorption process, the value of it should be less than 10 and higher than unity [62]. Table 4 shows the Freundlich isotherm model constants and respective correlation coefficients. The heat of the adsorption and the adsorbate-adsorbate interactions in an adsorption process were studied by *Temkin and Pyzhev* [63], and its equation is given as follows;

$$q_e = B_T \ln K_T + B_T \ln C_e \quad (5)$$

$$B_T = R_T b_T \quad (6)$$

Table 3: Isotherm parameters and correlation coefficients calculated by various adsorption isotherm model.

Model	Condition for applicability	Parameter	Value of parameters
Langmuir	Monolayer adsorption or homogenous surface	Q_m(mol g^{-1}) x 10^{-3}	16.80
		K_L (L g^{-1}) x 10^4	16.91
		R^2	0.992
Freundlich	Multi-layer adsorption or nonuniform distribution	$_{of}$ (mol g^{-1}) x 10^5	3.000
		1/n	0.602
		R^2	0.967
Temkin	Uniform distribution or heterogeneous surface	B_Tx 10^{-3}	17.53
		K_T(L g^{-1}) x 10^3	12.23
		R^2	0.979

Where B_T (J mol^{-1}) is the Temkin constant related to the heat of the adsorption, K_T (L/g) is the equilibrium binding constant corresponding to the maximum binding energy, R (8.314 J/mol K) is the universal gas constant and T (Kelvin) is the absolute solution temperature. The constants obtained for Temkin isotherm are shown in Table 4. The comparison of R -values obtained for the Freundlich and Langmuir isotherms revealed that Langmuir model is suitable to describe the adsorption of IC on supported melamine/ metal complexes, which emphasizes the formation of monolayer coverage of dye molecules on the surface of the adsorbent.

The essential feature of the Langmuir isotherm may be expressed in terms of a dimensionless constant called separation factor (R_L) which is given by the following equation.

$$R_L = 1/\left(1+K_L C_o\right) \quad (7)$$

The R_L values within the range $0< R_L<1$ indicate a favorable adsorption [64, 65]. In the present study, R_L values obtained were in the range of 0.037–0.051, indicating favorable adsorption of dye on supported melamine/ metal complexes**.**

Adsorption Kinetic study

The adsorption of organic compounds by natural materials in aqueous solution is a phenomenon with often complex kinetics because of their heterogeneous reactive surface. The kinetic study of the adsorption processes provides useful data about the efficiency of adsorption and feasibility of scale-up operations. Several kinetic models are available to examine the controlling mechanism of the adsorption process. Lagergren pseudo-first-order, pseudo-second-order, and intraparticle diffusion equations are the kinetic models applied to test the present experimental data. These models have widely been used for the adsorption of several adsorbates from aqueous solution [48]

Pseudo-first-order model

The adsorption kinetic data were described by the Lagergren pseudo- first order model, which describes the adsorption rate based on the adsorption capacity [66]. The Lagergren equation is commonly expressed as follows:

$$d_o/d_t = k_1\left(q_e - q_t\right) \quad (8)$$

Where q_e and q_t (mg/g) are the adsorption capacity at equilibrium and at time *t*, respectively, and k_1 (min^{-1}) is the rate constant of the pseudo-first order model. After definite integration by applying the conditions t = 0 to t = t and q_t = 0 to q_t = q_t the Eq. (9) becomes the following;

$$\log\left(q_e - q_t\right) = \log\left(q_e\right) - k_1/2.303t \quad (9)$$

k_1 is the first-order rate constant of adsorption. k_1 and q_e were determined from the slope and intercept of the plot of log (q_e - q_t) against t. Values of k_1 and the Pearson correlation coefficient are summarized in Table 5. The theoretical value of q_e characteristics of the Lagergren model gave a significantly different value in contrast to the experimental one that has a slightly lower correlation coefficient. Therefore, this model appears to be improper

Table 4: Parameters of pseudo-first order, pseudo-second order, and intraparticle diffusion models at different initial IC concentrations.

$[IC]_o x10^{-4}$ Mol\ L	Pseudo first order model for adsorption			Pseudo-second order model for adsorption				Intraparticle diffusion model for adsorption			
	$q_{ex}10^{-3}$ (mol/g)	k_1 (min^{-1})	R^2	$q_{e,cal}x10^{-3}$ mol/g	$q_{e,exp\,x}10^{-3}$ mol/g	k_2 mol^1g/min	R^2	$K_{p1}/\ 10^{-4}$ mol/g $min^{1/2}$	R^2	$K_{p2}\ /\ 10^{-4}$ mol/g $min^{1/2}$	R^2
1.1	22.02	0.022	0.981	24.93	22.02	0.245	0.996	3.70	0.991	-	-
1.2	23.00	0.040	0.980	26.36	25.00	0.264	0.998	32.2	0.998	7.03	0.993
1.4	26.80	0.050	0.989	32.80	31.25	0.576	0.997	35.1	0.994	19.4	0.992
1.5	28.83	0.081	0.991	36.47	34.83	0.737	0.995	64.1	0.995	6.13	0.985

for the current supported melamine/ metal complexes /dye system. Then the adsorption is not likely to be the first order reaction, even if this plot has a high correlation coefficient [67]. The variation in the rate of the adsorption should be proportional to the first power of concentration for strict surface adsorption. However, the relationship between the initial solute concentration and the rate of the adsorption will not be linear when the pore diffusion limits the adsorption process. The experimental data show a higher degree of nonlinearity and poor correlation coefficients for the pseudo-first order model.

Pseudo-second-order model

The adsorption kinetics may be described by the pseudo-second-order model [68], which is generally given as follows:

$$dq_t/dt = k_2\left(q_e - q_t\right)^2 \qquad (10)$$

Where k_2 (g/mg min) is the second-order rate constant of adsorption. After integration and applying boundary conditions $q_t = 0$ to $q_t = q_t$ at $t = 0$ to $t = t$, the integrated form of Eq.(11) becomes;

$$t/q_t = 1/k_2 q_e^2 + t/q_e \qquad (11)$$

The second-order rate constants are used to calculate the initial sorption rate, given by the following equation;

$$h = k_2 q_e^2 \qquad (12)$$

As mentioned above, the curve fitting plots of log ($q_e - q_t$) versus t does not show good results for the entire sorption period, while the plots of t/q_t versus t give a straight line for all the initial dye concentrations confirming the applicability of the pseudo-second-order equation. The values of k_2 and the equilibrium adsorption capacity, q_e, were calculated from the intercept and slope of the plots of t/q_t versus t, respectively. The R^2 values for the pseudo-second-order kinetic model were found to be higher, and the calculated q_e values were mainly close to the experimental data. This indicates that the adsorption of IC onto supported melamine/ metal complexes obeys the pseudo-second-order kinetic model for the entire sorption period. The transfer of the dyes from the solution phase into the pores of the adsorbent may also be considered as the rate controlling stage in the batch experiments under the rapid stirring condition.

Intra-particle diffusion model

The intra-particle diffusion model was applied to be able to see whether intra-particle diffusion could be the rate-limiting step in the adsorption process. In general, the dye sorption is governed by either the liquid phase mass transport rate or through the intra-particle mass transport rate. The adsorbate species are probably transported from the bulk of the solution into the solid phase with an intra-particle diffusion process, which is often the rate-limiting step in several adsorption processes. The possibility of intra-particle diffusion is explored by using the intra-particle diffusion model [69]. The adsorption process is a diffusive mass transfer process where the rate can be expressed in terms of the square root of time ($t^{0.5}$). The intra-particle diffusion model is expressed as following [70]:

$$q_t k_i t^{0.5} + C \qquad (13)$$

Where q_t (mg/g) is the fraction dye uptake at time t, k_i(mg/g $min^{1/2}$) is the intra-particle diffusion rate constant and C (mg g^{-1}) is the intercept. The values of C give an idea concerning the thickness associated with the boundary layer, i.e., the larger the intercept, the greater the contribution of the surface sorption at the rate controlling step. The plot of q_t versus$t^{0.5}$ will give k_i as slope nd C as intercept. The mechanism of any adsorption process may be assumed to involve the following three steps: (i) film diffusion; (ii) intra-particle or pore diffusion; (iii) sorption onto interior sites [71]. For intra particle diffusion plots, the first portion indicates a boundary layer effect at the initial stage of the adsorption. The second portion of the linear curve is the gradual adsorption stage the intra-particle diffusion is the rate limiting. In some cases, the third portion exists, which is the final equilibrium stage.

Adsorption thermodynamics

The adsorption mechanism often provides information on the type and level of interactions between the surface and the adsorbate. The dependence on temperature is certainly not sufficient reason to determine the type of adsorption. The type of adsorption can be realized via the thermodynamic parameters including the free energy of adsorption (ΔG_{ads}), the change in enthalpy of adsorption (ΔH_{ads}), and also the change in entropy (ΔS_{ads}). Both ΔH_{ads} and ΔS_{ads} were determined from the linear plot obtained between ln(qe/Ce) and 1/T (not shown) based on Eyring Eq. (14), [72]. In addition, the value of ΔG_{ads} was determined from Eq. (15).

$$\text{Ln}\,(q_e / C_e) = \Delta S_{ads}/ R - \Delta H_{ads}/ RT \quad (14)$$

$$\Delta G_{ads} = \Delta H_{ads} - T\,\Delta S_{ads} \quad (15)$$

The positive value of ΔH_{ads} (75.26 kJ/mol) indicates that the adsorption of IC dye onto supported / melamine complexes are endothermic. The positive value of ΔS_{ads} (315.45 J/mol K) refers to the increasing randomness at the solid/solution interface through the adsorption of the dye onto supported / melamine complexes [73]. The negative value of ΔG_{ads} (-96.295 kJ/mol) indicates the feasibility and spontaneity of adsorption.

CONCLUSIONS

The supported melamine/ metal complexes have been synthesized and used as an effective adsorbent for the removal of indigo carmine from aqueous solutions. The batch sorption process was dependent on some experimental parameters such as initial dye concentration, contact time, adsorbent dosage, and temperature. The isotherm parameters for the Langmuir, Freundlich and Temkin models were determined. The Langmuir isotherm model was found suitable to describe adsorption, suggesting monolayer coverage of dye molecules on the adsorbent surface. The dye adsorption followed the pseudo-second-order kinetics. Evaluation of thermodynamic parameters revealed that the adsorption process is endothermic and spontaneous. It can be concluded the present method is promising and can be considered as one of those methods devoted to treating the wastewater streams with low cost.

Received: May 7, 2016 ; Accepted: Jan. 9, 2017

REFERENCES

[1] Refat M.S., Adam A.- M.A., El-Sayed M.Y., Biomarkers Charge-Transfer Complexes of Melamine with Quinol and Picric Acid: Synthesis, Spectroscopic, Thermal, Kinetic and Biological Studies, *Arabian Journal of Chemistry*, **10**: S3482-S3492 (2014).

[2] Xu L.-F., Chen X.-L., Hu H.-M., Wang B.-C., Syntheses, Structures and Electrochemical Properties of Two Co-Crystal Copper(II) Melamine Complexes, *Journal of Molecular Structure*, **892**: 163-167 (2008).

[3] Zhang J., LiZ.-J., WenY.-H., KangY., ChengJ.-K., YaoY.-G., Syntheses and Structures of Two Novel Ag(I) Complexes: [μ_3-2-(4-pyridyl)Ethanesulfonato-N,O,O′]-Aqua-Silver(I) and Melamine-[2-(4-pyridyl)Ethanesulfonato-N]-Silver(I), *Journal of Molecular Structure*, **697**:185-189 (2004).

[4] Acharya S.N.G., Gopalan R.S., Kulkarni G.U., Venkatesan K., Bhattacharya S., Novel Organic Porous Solids with Channel and Layered Structures From 1, 3, 5-Triazine-2, 4, 6-Triaminehexaacetic Acid and Its Calcium Salt, *Chem. Commun.*,**15**: 1351-1352 (2000).

[5] Sharif M.A., Aghabozorg H., Shokrollahi A., Kickelbick G., Moghimi A., Shamsipur M. Novel Proton Transfer Compounds Containing 2,6-Pyridine dicarboxylic Acid and Melamine and Their PbII Complex: Synthesis, Characterization, Crystal Structure and Solution Studies, *Polish J. Chem*., **80**: 847-863 (2006).

[6] Feng W., Lv C., Yang L., Cheng J., Yan C., Determination of Melamine Concentrations in Dairy Samples, *LWT-food Science and Technology*, **47**:147-153 (2012).

[7] Kuang H., Chen W., Yan W., Xu L., Zhu Y., Liu L., Chu H., Peng C., Wang L., Kotov N.A., Xu C., Crown Ether Assembly of Gold Nanoparticles: Melamine Sensor, *Biosensors and Vioelectronics*, **26**: 2032-2037 (2011).

[8] Mauer L.J., Chernyshova A.A., Hiatt A., Deering A., Davis R., Melamine Detection in Infant Formula Powder Using Near- and Mid-Infrared Spectroscopy, *J Agric Food Chem.*, **57**: 3974-3980 (2009).

[9] Muñiz-Valencia R., Ceballos- Magaña S. G., Rosales-Martinez D., Gonzalo- Lumbreras R., Santos-Montes A., Cubedo- Fernandez-Trapiella A., Izquierdo- Hornillos R. C., Method Development and Validation for Melamine and Its Derivatives in Rice Concentrates by Liquid Chromatography. Application to Animal Feed Samples, *Anal. Bioanal.Chem*., **392**: 523-531 (2008).

[10] Xu X.M., Ren Y. P., Zhu Y.,Cai Z. X., Han J. L., Huang B. F., Zhu Y., Direct Determination of Melamine in Dairy Products by Gas Chromatography/ Mass Spectrometry with Coupled Column Separation, *Anal Chim. Acta*., **650**: 39-43 (2009).

[11] Yang G., Han H., Du C., Luo Z., Wang Y., Facile Synthesis of Melamine-based Porous Polymer Networks and Their Application for Removal of Aqueous Mercury Ions, *Polymer*, **51**: 6193-6202 (2010).

[12] Mooibroek T.J., Gamez P., The s-Triazine Ring, a Remarkable Unit to Generate Supramolecular Interactions, *Inorg. Chim. Acta*. ,**360**: 381-404 (2007).

[13] Steffensen M.B., Hollink E., Kuschel F., Bauer M., Simanek E.E., Dendrimers Based on [1,3,5]-Triazines, *J. Poly. Sci. Part A Poly. Chem.*, **44**: 3411- 3433 (2006).

[14] Zhang L., Li W., Zhang J., Li Z.-J., Qin Y.-Y., Cheng J.- K., Yao Y.- G., Anti Ferromagnetic Interactions in Melamine-Bridged Trinuclear Cobalt Complex, *Inorganic Chemistry Communications*,11: 8286-8293 (2008).

[15] Chen C., Yeh C.- W., Chen J.- D., Topology Analysis and Nonlinear-Optical-Active Properties of Luminescent Metal-Organic Framework Materials Based on Zinc/Lead Isophthalates, *Polyhedron*, **25**:1307- 1312 (2006).

[16] Wiles A. B., Bozzuto D., Cahill C. L., Pike R. D., Copper (I) and (II) Complexes of Melamine, *Polyhedron*, **25**: 776-782 (2006).

[17] Zhang X.-L., Chen X.-M., Copper (I) and (II) Complexes of Melamine, *Crystal Growth & Design*, **5**: 776-782 (2005).

[18] Ye B.H., Infinite Water Chains Trapped in an Organic Framework Constructed from Melamine with 1,5-Naphthalenedisulfonic Acid via Hydrogen Bonds, *Crystal Growth & Design*, **5**: 1609- 1616 (2005).

[19] YuY.-Q., LuC.-Z., He X., Chen S.-M., Zhang Q.-Z., Chen L.-J., Yang W.-B., Synthesis, Structure and Fluorescent Property of a Novel Inorganic–Organic Zinc Compound, *J. Chem. Cryst.*, **34**: 905-909 (2004).

[20] Schwab M.G., Fassbender B., Spiess H.W., Thomas A., Feng X., Müllen K., Catalyst-Free Preparation of Melamine-Based Microporous Polymer Networks through Schiff Base Chemistry, *J. Am. Chem. Soc*., **131**: 7216-7217 (2009).

[21] Li Y.-H., Sun D., Luo G.-G., Liu F.-J., Hao H.-J., Wen Y.-M., Zhao Y., Huang R.-B., Zheng L.-S., Two Ag(I) Coordination Polymers Derived From Melamine and Dicarboxylates: Syntheses, Crystal Structures and Thermal Stabilities, *J. of Molecular Structure*, **1000**: 85- 91 (2011).

[22] Li Y., Gao Y.,Cao Y., Li H., Electrochemical Sensor for Bisphenol A Determination Based on MWCNT/Melamine Complex Modified GCE, *Sensors and Actuators B: Chemical*, **171**: 726- 733 (2012).

[23] Saggioro E.M., Oliveira A.S., Buss D.F., Photo-Decolorization and Ecotoxicological Effects of Solar Compound Parabolic Collector Pilot Plant and Artificial Light Photocatalysis of Indigo Carmine Dye, *Dye Pigment*, **113**: 571- 580 (2015).

[24] Barka N., Assabbane A., Nounah A., Ichou Y.A., Photocatalytic Degradation of Indigo Carmine in Aqueous Solution by TiO_2-Coated Non-Woven Fibres, *J Hazard Mater*.,**152**:1054-1059 (2008).

[25] Jeffords D.L., Lance P.H., Dewolf WC Severe Indigo. Severe Hypertensive Reaction to Indigo Carmine, *Urology*, **9**:180–181 (1977).

[26] Zainal Z., Hui L.K., Hussein M.Z., Taufiq-Yap Y.H., Abdullah A.H., Ramli I., Removal of Dyes Using Immobilized Titanium Dioxide Illuminated by Fluorescent Lamps, *J Hazard Mater*, **125** : 113-120 (2005).

[27] Martínez-Orozco R.D., Rosu H.C., Lee S.W., Rodríguez-González V., Thin Extractive Membrane for Monitoring Actinides in Aqueous Streams, *J. Hazard Mater*., **263**: 53- 60 (2013) .

[28] Mededovic S., Takashima K., Decolorization of Indigo Carmine Dye by Spark Discharge in Water, *Int J Plasma Env Sci Technol*., **2**: 56-66 (2008).

[29] Dogdu G., Yalcuk A., Indigo Dyeing Wastewater Treatment by Eco-Friendly Constructed Wetlands Using Different Bedding Media, *Desalination and Water Treatment*, **57**: 15007-15019 (2016).

[30] Hammami S., Oturan M.A., Oturan N., Comparative Mineralization of Textile Dye Indigo by Photo-Fenton Process and Anodic Oxidation Using Boron-Doped Diamond Anode, *Desalin Water Treat.*, **45**: 297-304 (2012).

[31] Lorimer J.P., Mason T.J., Plattes M., Phull S.S., Dye Effluent Decolourisation Using Ultrasonically Assisted Electro-Oxidation, *Ultrason Sonochem*., **7**: 237-242 (2000).

[32] Galindo C., Jacques P., Kalt A., Photochemical and Photocatalytic Degradation of an Indigoid Dye: a Case Study of Acid Blue 74 (AB74), *J Photochem Photobiol A Chem*., **141**: 47- 56 (2001).

[33] Meier R.J., Maple J. R., Hwang M.-J., Hagler A., Molecular Modeling Urea- and Melamine-Formaldehyde Resins. 1. A Force Field for Urea and Melamine, *J. Phys. Chem*., **99**: 5445- 5456 (1995).

[34] Schneider J.R., Schrader B., Measurement and Calculation of the Infrared and Raman Active Molecular and Latice Vibrations of the Crystalline Melamine(1,3,5-triamino-s-triazine), *J. Mol. struct*, **29**: 1-14 (1975).

[35] Chen W. -C., Wu S. -Y., Liu H. -P., Chang C. -H., Chen H.-Y., Chen H. -Y., Tsai C.-H., Chang Y.-C., Tsai F.-J., Man K.-M., Liu P.-L., Lin F. -Y., Shen J. -L., Lin W.-Y., ChenY. -H., Identification of Melamine/ Cyanuric Acid-Containing Nephrolithiasis by Infrared Spectroscopy, *Journal of Clinical Laboratory Analysis*, **24**: 92- 99 (2010).

[36] Costa L., Camino G., Thermal Behaviour of Melamine, *J. Therm. Anal. Cal*., **34**:423- 429 (1988).

[37] Kandelbauer A., Despres A., Pizzi A., Taudes I., Testing by Fourier Transform Infrared Species Variation During Melamine–Urea–Formaldehyde Resin Preparation, *J. Appl. Polym. Sci*., **106**: 2192-2197 (2007).

[38] Wang Z., Lv P., Hu Y., Hu K., Thermal Degradation Study of Intumescent Flame Retardants by TG and FTIR: Melamine Phosphate and Its Mixture with Pentaerythritol, *J. Anal. Appl. Pyrolysis*, **86**: 207-214 (2009).

[39] Costa L., Camino G., Thermal Behaviour of Melamine, *J. Therm. Anal*., **34**: 423- 429 (1988).

[40] Bellamy L.J., "The Infra-Red Spectra of Complex Molecules", Chapman and Hall, London, (1975).

[41] Okoronkwo1 E.A., Imoisili1P.E., Olusunle S.O., Extraction and Characterization of Amorphous Silica from Corn Cob Ash by Sol-Gel Method, *Chemistry and Materials Research*, **3**: 68- 75 (2013).

[42] Javed S. H., Shah F. H., Manasha M., Extraction of Amorphous Silica From Wheat Husk by Using $KMnO_4$, *JFET*, **18**: 39- 46 (2011).

[43] Prakash N. J., "Preparation and Characterization of Bioactive Silica-Based Ceramics Derived from Rice Husk Ash" PhD Thesis. National Institute of Technology, Rourkela, (2010).

[44] Lei M., Zhao H.Z., Yang H., Song B., Tang W.H., Synthesis of Transition Metal Carbide Nanoparticles Through Melamine and Metal Oxides, *Journal of the European Ceramic Society*,**28**:1671- 1677 (2008).

[45] Jurgens B., Irran E., Senker J., Kroll P., Muller H., Schnick W., Melem (2,5,8-Triamino-tri-s-triazine), an Important Intermediate during Condensation of Melamine Rings to Graphitic Carbon Nitride: Synthesis, Structure Determination by X-ray Powder Diffractometry, Solid-State NMR, and Theoretical Studies, *J. Am. Chem. Soc.*, **125**: 10288- 10300 (2003).

[46] Camino G., Costa L., Luda di Cortemiglia M.P., Overview of Fire Retardant Mechanisms, *Polym. Degrad. Stab*., **33**: 131- 154 (1991).

[47] Prabhumirashi L. S., Khoje J. K., TGA and DTA Studies on en and Tmn Complexes of Cu(II) Chloride, Nitrate, Sulphate, Acetate and Oxalate, *Thermochimica Acta*, **383**: 109- 118 (2002).

[48] Elsherbiny A.S., Salem M.A., Ismail A.A., Influence of the Alkyl Chain Length of Cyanine Dyes on Their Adsorption by Na^+-Montmorillonite From Aqueous Solutions, *Chemical Engineering Journal*, **200**: 283- 290 (2012).

[49] Ramakrishna K.R., Viraraghavan T., Volatile Fatty Acid Production in Aerobic Thermophilic Pre-Treatment of Primary Sludge, *Water Sci. Technol*., **36**: 189- 196 (1997).

[50] DÕgan M., Alkan M., Demirbas O., Ozdemir Y., Ozmetin C., Adsorption Kinetics of Maxilon Blue GRL Onto Sepiolite From Aqueous Solutions, *Chem. Eng. J*., **124**:89-101 (2006).

[51] Mall I.D., Srivastava V.C.,Agarwal N.K., Mishrab I.M., Removal of Congo Red From Aqueous Solution by Bagasse Fly Ash and Activated Carbon: Kinetic Study and Equilibrium Isotherm Analyses, *Chemosphere*, **61**: 492-501 (2005).

[52] Vautier M., Guillard C., Herrmann J.M., Photocatalytic Degradation of Dyes in Water: Case Study of Indigo and of Indigo Carmine, *J. Catal*., **201**: 46-59 (2001).

[53] Ramadan A.M., El-Naggar M.M., Synthesis, Characterization and Demonstration of Superoxide Dismutase-Like Activity of Copper(II) Chloride, Bromide, Nitrate, Thiocyanate, Sulphate, and Perchlorate Complexes with 2-Methyl-Amino Pyridine, *J. Inorg. Biochem*, **63**: 143- 153 (1996).

[54] Marcus Y., "Ion Properties" Marcel Dekker, New York, (1997).

[55] Johanson U., Marandi M.,Tamm T., Tamm J., Comparative Study of the Behavior of Anions in Polypyrrole Films, *Electrochem. Acta*, **50**: 1523-1528 (2005).

[56] Ghaedi M., Sadeghian B., Amiri Pebdani A., Sahraei R., Daneshfar A.,Duran C., Kinetics, Thermodynamics and Equilibrium Evaluation of Direct Yellow 12 Removal by Adsorption Onto Silver Nanoparticles Loaded Activated Carbon, *Chemical Engineering Journal*, **187**: 133-141 (2012).

[57] Chiou M.S., Li H.Y., Equilibrium and Kinetic Modeling of Adsorption of Reactive Dye on Cross-Linked Chitosan Beads, *J. Hazard. Mater*., **93**: 233-248 (2002).

[58] Langmuir I., The Adsorption of Gases on Plane Surfaces, Mica and Platinum, *J. Am. Chem. Soc*., **40**: 1361- 1403 (1918).

[59] Li Q., Yue Q.Y.,SuY., Gao B.Y., Sun H.J., Equilibrium, Thermodynamics and Process Design to Minimize Adsorbent Amount for the Adsorption of Acid Dyes Onto Cationic Polymer-Loaded Bentonite, *Chem. Eng. J*., **158**: 489- 497 (2010).

[60] Langmuir I., The Constitution and Fundamental Properties of Solids and Liquids: Part I Solids, *J. Am. Chem. Soc.*, **38**: 2221-2295 (1916).

[61] Abdelwahab O., Evaluation of the Use of Loofa Activated Carbons as Potential Adsorbents for Aqueous Solutions Containing Dye, *Desalination*, **222**: 357-367 (2008).

[62] Chilton N., Losso J.N., Marshall W.E., Freundlich Adsorption Isotherms of Agricultural by-Product-Based Powdered Activated Carbons in a Geosmin–Water System, *Bioresour. Technol*., **85**: 131-135 (2002).

[63] Temkin M.J., Pyzhev V., Recent Modification to Langmuir Isotherms, *Acta Physiochim. USSR*, **12**: 217- 222 (1940).

[64] Ai L., Huang H.,Chen Z., Wei X., Jiang J., Activated Carbon/$CoFe_2O_4$ Composites: Facile Synthesis, Magnetic Performance and Their Potential Application for the Removal of Malachite Green From Water,*Chemical Engineering Journal*, **156**: 243-249 (2010).

[65] Jain M., Garg V.K., Kadirvelu K., Adsorption of Hexavalent Chromium From Aqueous Medium Onto Carbonaceous Adsorbents Prepared From Waste Biomass, *Journal of Environmental Management*, **91**: 949- 957 (2010).

[66] Lagergren S., Adsorptive Treatment of Brewery Effluent Using Activated Chrysophyllum Albidium Seed Shell Carbon, Zurtheorie der Sogenannten Adsorption Gelosterstoffe, *Kung Sven. Veten.Hand.*, **24**: 1- 10 (1898).

[67] Iqbal M.J., Ashiq M.N., Adsorption of Dyes from Aqueous Solutions on Activated Charcoal, *J. Hazard. Mater*.**,139:** 57-66 (2007).

[68] Ho Y.S., McKay G., Wase D.A.J., Foster C.F., Study of the Sorption of Divalent Metal Ions on to Peat, *Adsorpt. Sci. Technol*., **18**: 639-650 (2000).

[69] Ruthven D.M, Loughlin K.F., The Effect of Crystallite Shape and Size Distribution on Diffusion Measurements in Molecular Sieves, *Chem. Eng. Sci.*, **26**: 577-584 (1971).

[70] Pignatello J.J., Ferrandino F.J., Huangm L.Q., Elution of Aged and Freshly Added Herbicides From a Soil, *Environ. Sci. Technol*., **27**: 1563-1571 (1993).

[71] Arami M., Limaee N.Y., Mahmoodi N.M., Tabrizi N.S., Equilibrium and Kinetics Studies for the Adsorption of Direct and Acid Dyes from Aqueous Solution by Soy Meal Hull, *J. Hazard. Mater*., **135**: 171-179 (2006).

[72] Laidler K.J., Meiser J.M., "Physical Chemistry, Houghton Mifflin", New York, 852 (1999).

[73] Raji C., Anirudhan T.S., Chromium (VI) Adsorption by Sawdust Carbon: Kinetics and Equilibrium, *Ind. J. Chem. Technol*. **4**: 228-236 (1997).